


ORIGINAL RESEARCH ARTICLE

RKI-1447 suppresses colorectal carcinoma cell growth via disrupting cellular bioenergetics and mitochondrial dynamics

Liyi Li^{1,2}  | Qin Chen³ | Yaojun Yu² | Hui Chen¹ | Mingdong Lu¹ |
Yingpeng Huang¹ | Pihong Li¹ | Hong Chang¹¹General Surgery Department, Shandong Provincial Hospital Affiliated to Shandong University, Ji'nan, Shandong, China²General Surgery Department, Second Affiliated Hospital of Wenzhou Medical University, Wenzhou, Zhejiang, China³Department of Intensive Care, First Affiliated Hospital of Wenzhou Medical University, Wenzhou, China**Correspondence**Hong Chang, Provincial Hospital affiliated to Shandong University, No. 324, Jingwu Road, Ji'nan, 250000 Shandong, China.
Email: changhong@sdu.edu.cn**Funding information**

Key Research and Development Program of Shandong Province, Grant/Award Number: 2015GGH318017

Abstract

Accumulated evidence suggested the importance of the Rho/Rho-kinase (ROCK) signaling pathway in cancer proliferation and invasion. However, its role in colorectal carcinoma (CRC) is not well understood. This study evaluated the effect of ROCK signaling pathway on CRC behavior on the basis of a novel Rho/ROCK inhibitor RKI-1447. Here, we found RKI-1447 could drastically suppress HCT-8 and HCT-116 cell growth and promoted apoptosis. Our in vitro data indicated suppressed cytoskeletal dynamics induced by RKI-1447 inhibition on mitochondrial respiration, which was evidenced by basal and maximal respiration rates, and ATP production. Simultaneously, cellular basal and maximal glycolytic rates, and glycolytic capacity were also reduced in response to RKI-1447. Moreover, RKI-1447 caused excessive reactive oxygen species generation and membrane depolarization as well as activated ER-stress. We also demonstrated CHOP is essential for RKI-1447 induced cell apoptosis. Finally, we proved inhibition of ROCK by RKI-1447 could effectively inhibit CRC growth in vivo. Taken together, this study demonstrated that inhibition of ROCK signaling pathway by RKI-1447 could suppress CRC via cytoskeleton associated mitochondrial dysfunction and cellular bioenergetics disruption. Our data suggest RKI-1447 may be an attractive antitumor drug candidate for the treatment of CRC.

KEYWORDS

cellular bioenergetics, colorectal carcinoma, ER-stress, mitochondrial dysfunction, RKI-1447

1 | INTRODUCTION

Colorectal carcinoma (CRC) is a common malignancy that has high incidence and mortality rates, with nearly 609,051 died from CRC annually (Ferlay et al., 2015; Gemma, Binefa, & Francisco, 2014; Wang et al., 2017). Although diagnostic biomarkers and therapeutic strategies are emerging, the outcome of patients with CRC remains poor. It is urgent to develop novel therapeutic strategies to improve the prognosis of patients with CRC.

Multiple works has demonstrated that Rho-kinase (ROCK) was drastically overexpressed in various cancer types and played crucial roles in cancer initiation and progression. ROCK includes two isoforms ROCK1 and ROCK2 (Chen et al., 2002), which are downstream effectors of Rho

A. Growing evidence demonstrated that ROCK plays a central role in multiple biological processes including stress-fiber formation and contraction, cell adhesion, migration, and invasion (Riento & Ridley, 2003; Vega & Ridley, 2008). The C terminus of ROCK contains an unconventional PH domain with an internal cysteine-rich motif (Leung, Chen, Manser, & Lim, 1996). In addition, the conserved catalytic kinase domain has been proved to regulate actin cytoskeleton remodeling in the process of cell division (Di Cunto et al., 2000; Jin, Shimizu, Balasubramanyam, Epstein, & H, 2000; Leung, Chen, Tan, Manser, & Lim, 1998; Madaule et al., 1998). The regulation of the catalytic activity of serine/threonine protein kinases often involves phosphorylation in the activation loop and the hydrophobic motif C-terminal to the kinase domain by auto-phosphorylation and/or phosphorylation by a heterologous kinase

(Alessi & Cohen, 1998; Newton, 1997; Vanhaesebroeck & Alessi, 2000). Several works have investigated the essential role of ROCK in CRC (Zeng et al., 2015) previous work has demonstrated activation of Rho and ROCK is indispensable for colorectal cancer cell metastasis (Voorneveld et al., 2014). Recently, RhoA/ROCK/ Myosin light chain pathway is crucial for Vincristine mediated colorectal cancer cells cell migration and invasion (Jin et al., 2016). Interestingly, recent findings demonstrated that ROCK1 phosphorylated mitochondrial DRP1 to induce mitochondrial fission. In addition, knockdown of ROCK1 promoted Reactive oxygen species (ROS) generation and thus led to apoptosis (Wenjia Wang et al., 2012; Yundi Shi et al., 2018). These data suggested the involvement of ROCK1 on mitochondrial associated bioenergetics and mitochondrial dynamics.

Given the importance of ROCK in cancer cells and the involvement of ROCK in mitochondrial function, it is interesting to investigate whether the regulation of mitochondrial function by ROCK is essential for colorectal cancer cell survival or proliferation. Because RKI-1447 is a highly potent ROCK inhibitor and its function on CRC remains unknown, we asked if RKI-1447 could inhibit CRC growth via alteration of mitochondrial associated bioenergetics and metabolism.

In this study, we confirmed ROCK1/2 inhibitor RKI-1447 exhibited effective anticancer activity in CRC. And this could be reasoned to the fact that RKI-1447 regulates cellular bioenergetics and induces apoptosis through disrupting mitochondrial respiration and activating ER-stress. Increased CHOP contributes to RKI-1447 induced CRC apoptosis. This can be the mechanism of RKI-1447 suppressed CRC cancer cell growth, and highlights the promising antitumor activity of RKI-1447.

2 | MATERIAL AND METHODS

2.1 | Reagents and antibodies

RKI-1447 was obtained from Selleck Co. (Shanghai, China). Horseradish peroxidase (HRP)-conjugated anti-rabbit, anti-mouse immunoglobulin G, MTT Cell Proliferation, and Cytotoxicity Assay kit, ROS Assay Kit (DCFH-DA) and mitochondrial membrane potential (MMP) Assay kit (JC-1) were all obtained from Beyotime Biotech (Jiangsu, China). Annexin-V (FITC) Apoptosis Detection kit was obtained from BD Biosciences (Franklin Lakes, NJ). BCA Protein Assay Kit and Pierce ECL Western blot analysis Substrate were both obtained from Thermo Fisher Scientific, Inc. (Waltham, MA). Monoclonal antibody against β -actin was from Abmart (Shanghai, China). Polyclonal antibody against PARP, caspase-3, cleaved caspase-3, OPA1, ATF4, ATF6, OMA1 PERK, p-eIF 2 α , and eIF2 α were all obtained from Cell Signaling Technology, Inc. (Beverly, MA).

2.2 | Cell lines and cell culture

The CRC cell lines, HCT-8, HCT116, SW480, and DLD1 were both purchased from the Cell Bank of the Chinese Academy of Sciences (Shanghai, China). The cells were grown in DMEM medium

supplemented with 10% fetal bovine serum (FBS; both from Invitrogen, Carlsbad, CA) and antibiotics (100 U/ml penicillin and 100 μ g/ml streptomycin) at 37°C in a humidified atmosphere of 5% CO₂.

2.3 | MTT assay

For MTT assay, HCT-8 and HCT116 cells were seeded into 96-well plates at a density of 2×10^3 cells/well and incubated at 37°C in a humidified atmosphere of 5% CO₂ overnight. Next day, HCT-8 and HCT116 cells were treated with R1-1447(0, 10, 20, 40, 80, 160, 320 μ M) for 24 hr, respectively. The cells were stained with MTT reagent (5 mg/ml) for 4 hr, and the crystals produced were dissolved with DMSO. Once the crystals were dissolved completely, absorbance at 570 nm was measured by the plate reader (Thermo Fisher Scientific, Inc.).

2.4 | Colony formation assay

HCT-8 and HCT-116 cells were counted, and a total of 600 cells per well were seeded into six-well plates and incubated at 37°C overnight. Then incubating medium was replaced with fresh medium containing a gradient concentration of RKI-1447 (0, 20, 40, 80 μ M) and cultured at 37°C, 5% CO₂ for another 14 days. Next, the cells were washed with pre-warmed phosphate-buffered saline (PBS) for three times, then fixed with 4% paraformaldehyde (PFA) and stained with Giemsa solution for 15 min, followed by washing with pre-warmed PBS for three times, and counted by Image Plus 6.0 software.

2.5 | Apoptosis analysis

HCT-8 and HCT116 cells were seeded in a six-well plate at a density of 2×10^5 cells/well and treated with RKI-1447 (0, 20, 40, 80 μ M), respectively. After treatment for 24 hr, the cells were collected, washed twice with ice-cold PBS, and subsequently stained with Annexin V-FITC/PI for 20 min by incubation in the dark at room temperature. The samples were subsequently analyzed immediately using a BD Accuri C6 flow cytometer (BD Biosciences).

2.6 | Reactive oxygen species determination

DCFH-DA detection kit was used to measure intracellular ROS levels according to manufacturer's instructions. HCT-8 and HCT-116 cells were treated with RKI-1447 (0, 20, 40, 80 μ M), respectively. 24 hr post treatment, cell samples were collected and incubated with FBS-free DMEM medium containing 10 mM DCFH-DA at 37°C for 15 min in the dark. Then, the cells were washed with FBS-free DMEM medium for once and resuspended with 200 μ l FBS-free DMEM medium. Cellular total ROS level was analyzed by flow cytometry within 30 min.

2.7 | JC-1 fluorescence analysis

MMP was measured by JC-1 staining as previously described. Briefly, HCT-8 and HCT116 cells treated with RKI-1447 (0, 20, 40, 80 μ M) were incubated with 2.0 μ M JC-1 probe for 20 min at 37°C in the dark. The excess JC-1 probe was removed by washing cells with warm PBS and pelleted by centrifugation. Cell pellets were resuspended in 500 μ l PBS and MMP was assayed by flow cytometry.

2.8 | Western blot analysis

HCT-8 and HCT116 cells were treated with RKI-1447 (0, 20, 40, 80 μ M) for 24 hr, then trypsinized and collected in 1.5 ml tubes, lysed in RIPA buffer (50 mM Tris-HCl, pH 7.4, 1% Triton X-100, 1% sodium deoxycholate, 0.1% SDS, 150 mM NaCl) supplemented with protease inhibitor cocktail tablet, NaF (1 mM) and Na_3VO_4 (1 mM) for 15 min on ice and centrifuged at 18,000 \times g for 20 min at 4°C. Equal amount of protein from total lysates were resolved by 15% SDS-PAGE, the separated proteins were transferred onto nitrocellulose membrane (Bio-Rad Laboratories, Inc., Hercules, CA) in Tris-glycine buffer. Blots were blocked at room temperature for 1.5 hr in blocking buffer (5% nonfat milk in TBST) on a shaker and then incubated overnight at 4°C with primary antibodies as indicated in the figures. After washing, membranes were incubated for 1 hr with an anti-mouse or anti-rabbit IgG-HRP and detected with the ECL system. The optical density was quantified by the ImageJ software (National Institutes of Health, Bethesda, MA).

2.9 | Cellular bioenergetics analysis

The Seahorse XF96 Extracellular Flux Analyzer (Seahorse Bioscience, North Billerica, MA) was used to assay mitochondrial bioenergetics by measuring cellular oxygen consumption rate (OCR) and extracellular acidification rate (ECAR). For OCR determination, the optimal number of cells for each OCR measurement was determined to be 20,000/ well. HCT-8 and HCT116 cells treated with RKI-1447 of different concentrations (0, 20, 40, 80 μ M) were incubated in a 37°C, 5% CO_2 incubator, and the calibrator plate was equilibrated in a non- CO_2 incubator overnight. Next day, the medium was changed to Dulbecco's modified Eagle's medium (unbuffered DMEM, 25 mM glucose, 1 mM glutamine, 1 mM sodium pyruvate) and equilibrated in a 37°C CO_2 -free prep station for 40 min. Then the following chemicals were injected sequentially into the cell plates, followed by measurement of OCR: (a) oligomycin, an ATP synthase inhibitor (1 μ M final concentration), (b) carbonylcyanide *p*-trifluoromethoxyphenylhydrazone (FCCP), an ETC accelerator which causes maximal respiration rate (1 μ M final concentration), (c) rotenone plus antimycin A which are mitochondrial complex I and III inhibitors respectively (1 μ M final concentration of each). For ECAR detection, RKI-1447 pretreatment was the same with OCR detection. The compound for ECAR determination is glucose (10 mM), Oligomycin (1 μ M) and 2-DG (100 mM). The OCR and ECAR measurement for

each RKI-1447 treatment group was performed in triplicate, in three independent experiment.

2.10 | Cell transfection

HCT-8 cells were seeded into 6-cm dishes and cultured at 37°C, 5% CO_2 overnight. The cells were transfected with siRNA targeting CHOP by lipofectamine 2000. The sequences of siRNA are as below: siRNA for CHOP: 5'-GAGCUCUGAUUGACCGAAUTT-3' (forward), 5'-AGAGCGCAGCCACGG ACGCTT-3' (reverse). The cells transfected with CHOP were used for further experiments.

2.11 | Tumor xenograft assay

Male BALB/C mice were purchased from Shanghai Laboratory Animal Center, CAS (Shanghai, China) and housed in a specific pathogen-free (SPF) environment. HCT-8 cells (3×10^6 cells in 50 μ l medium mixed with 50 μ l Matrigel) were injected subcutaneously into the flanks of 5-week-old nude mice ($n = 8$). Tumor length (L) and width (W) were measured every 2 days with calipers, and the tumor volume (V) was calculated ($V = 1/2 (L \times W^2)$). When tumor volumes reached approximately 250 mm^3 , mice were randomly divided into two groups. One group was intraperitoneally injected with RKI-1447 (100 mg/kg) and control group was treated with 0.9% NaCl. After treatment for 12 days, mice were killed, and the tumors were dissected out and weighed, and the tumors were dissected out and weighted. Tumors tissues were homogenized and lysed for western blot analysis analysis, as described in section 2.8. All animal procedures were conducted according to the guidelines approved by the Institutional Animal Care and Use Committee of Wenzhou Medical University.

2.12 | Statistical analysis

All statistical analyses were carried out using SPSS version 16.0 statistical software package (SPSS Inc., Chicago, IL) and presented with Graph Pad Prism version 5.0 software (Graph Pad Software, Inc., La Jolla, CA). Student's *t* test was used to compare the difference of means from two different treatment groups. All *p* values are two-sided, and $p < .05$ was considered as a statistically significant difference. Error bars represent the standard deviation of the data from three separate experiments.

3 | RESULTS

3.1 | RKI-1447 suppresses CRC cell growth and promotes apoptosis

Rho-associated kinases ROCK1 and ROCK2 are critical for cancer cell migration and invasion, suggesting they may be useful therapeutic targets. RKI-1447 was discovered as a potent small molecule inhibitor of ROCK1 and ROCK2. Crystal structures of the RKI-1447/ROCK1 complex revealed that RKI-1447 is a Type I kinase inhibitor

that binds the ATP binding site through interactions with the hinge region and the DFG motif. Antitumor activity of RKI-1447 was recently investigated in breast cancer and clear cell renal carcinoma. Rho-associated kinases were reported to promote CRC cell migration and invasion. We asked whether RKI-1447 could suppress CRC growth. To test our hypothesis, we assessed the anticancer activity of RKI-1447 in CRC cell lines. First, we measured viability under RKI-1447 treatment. In Figure 1a, we found that the HCT-8 and HCT-116 viability was drastically decreased in a dose-dependent manner. We also detected the antitumor activity in other CRC cell lines SW480 and DLD1 and found the same effects (Figure S1). In addition, colony formation data showed RKI-1447 could reduce cell clone number in both HCT-8 and HCT-116 cells. Furthermore, apoptosis was induced upon RKI-1447 treatment (20, 40, 80 μ M) (Figure 1c,d), in a dose-dependent manner. Consistently, cleavage of PARP and caspase 3 were found to be increased in HCT-8 and HCT-116 cells treated with RKI-1447 (Figure 1e). These data indicated that RKI-1447 possesses antitumor activity in CRC cells.

3.2 | Decreased mitochondrial respiration is responsible for RKI-1447 induced CRC suppression

Mitochondria are the energy center of mammalian cells, almost 90% ATP were produced by oxidative phosphorylation (OXPHOS; Stefano & Kream, 2015; Vyas, Zaganjor, & Haigis, 2016). Multiple works have demonstrated the correlation between mitochondrial function and cancer. Here, we found the overall OCR was dose-dependently repressed by RKI-1447 treatment in both HCT-8 and HCT-116 cells (Figure 2a). To elaborate on the alteration of OCR by RKI-1447 treatment, we assessed the three mitochondrial respiration indexes including rates of basal respiration and maximal respiration, and spare respiration capacity. We found basal respiration rate, maximal respiration rate and ATP production were all decreased in RKI-1447 treated cells (Figure 2b–d, respectively). These data indicated that RKI-1447 could suppress mitochondrial respiration which would result in energy deficiency.

3.3 | RKI-1447 drastically represses aerobic glycolysis in CRC cells

Previous works have emphasized the importance of cellular metabolic alteration to tumor initiation and progression. Warburg effect described enhanced aerobic glycolysis is crucial for malignant behavior (Liberti & Locasale, 2016). So we asked whether RKI-1447 could inhibit aerobic glycolysis in CRC cells. To validate the effects of RKI-1447 on aerobic glycolysis, Seahorse XF-96 bioenergetics analyzer was utilized to detect the change of extracellular acidification rate (ECAR). As shown in Figure 3a, significant reduction of overall aerobic glycolysis was found in RKI-1447 treated HCT-8 and HCT-116 cells. We also assessed the basal glycolytic rate, maximal glycolytic rate and glycolytic capacity (Figure 3b–d, respectively). On the basis of the data of mitochondrial respiration and aerobic glycolysis, we suggest that the suppression on cellular

bioenergetics by RKI-1447 is responsible for the anticancer activity of RKI-1447.

3.4 | RKI-1447 induced mitochondrial depolarization activates OPA1 cleavage, leading to ER-stress associated apoptosis in HCT116 and HCT-8 cells

On the basis of the data of mitochondrial respiration suppression, we asked whether RKI-1447 could disrupt other mitochondrial functions. To dissect the mechanism, first, we measured the cellular ROS levels by flow cytometry. As shown in Figure 4a, we found excessive ROS generation in RKI-1447 treated cells which could enhance oxidative damage and induce apoptosis (Matés, Segura, Alonso, & Márquez, 2012; Poillet-Perez, Despouy, Delage-Mourroux, & Boyer-Guittaut, 2015). Furthermore, we also determined another index of mitochondrial function: mitochondrial membrane potential (MCP). Consistently, MCP was drastically decreased under RKI-1447 treatment, which indicated that RKI-1447 results in mitochondrial depolarization (Figure 4b). Multiple works have demonstrated that reduction of MCP would result in the release of pro-apoptosis factors from mitochondria to cytoplasm or nucleus which finally initiates apoptosis (Ly, Grubb, & Lawen, 2003; Suzuki-Karasaki, Suzuki-Karasaki, & Uchida, 2014). It is well validated that excessive ROS generation and mitochondrial depolarization disrupt mitochondrial dynamics, so we visualized mitochondria by Mito-tracker and observed higher degree of mitochondrial fragmentation upon RKI-1447 treatment in HCT-8 cells (Figure 4c). Moreover, we found mitochondrial dynamin-like 120 kDa protein OPA1 was cleaved in response to RKI-1447 treatment (Figure 4d). Previous work has validated that OPA1 localizes to the inner mitochondrial membrane, where it regulates mitochondrial fusion and cristae structure. OPA1 mediates mitochondrial fusion in cooperation with mitofusins 1 and 2, and participates in cristae remodeling through oligomerization of two L-OPA1 and one S-OPA1, which then interact with other protein complexes to alter cristae structure. OPA1 regulates cristae function also contributes to its role in oxidative phosphorylation and apoptosis, as it is required to maintain mitochondrial activity during low-energy substrate availability (Banerjee & Chinthapalli, 2014; Kushnareva et al., 2013; Quirós, Ramsay, & López-Otín, 2013). Here, we found OPA1 was cleaved to S-OPA1. Consistently, we found OPA1 cleavage was increased by RKI-1447, the former was essential for OPA1 cleavage (Figure 4d,e). As OPA1 stability is crucial to mitochondrial homeostasis, we suggested that RKI-1447 activated OPA1 cleavage explains why RKI-1447 disturbed mitochondrial respiration. MPT regulates cristae junction (CJ) remodeling in ER stress-induced cytochrome c-dependent apoptosis, and mitochondrial electron transport is involved for this process (Zhang, Lu, Whiteman, Chance, & Armstrong, 2008). So we evaluated the change of ER stress associated molecules: p-eIF2 α and CHOP expression under RKI-1447 treatment. In Figure 4d,e, p-eIF2 α and CHOP levels were both increased by RKI-1447. These data indicated that RKI-1447 activates mitochondrial depolarization, which then induces OPA1 cleavage, and finally promotes ER-stress associated apoptosis.

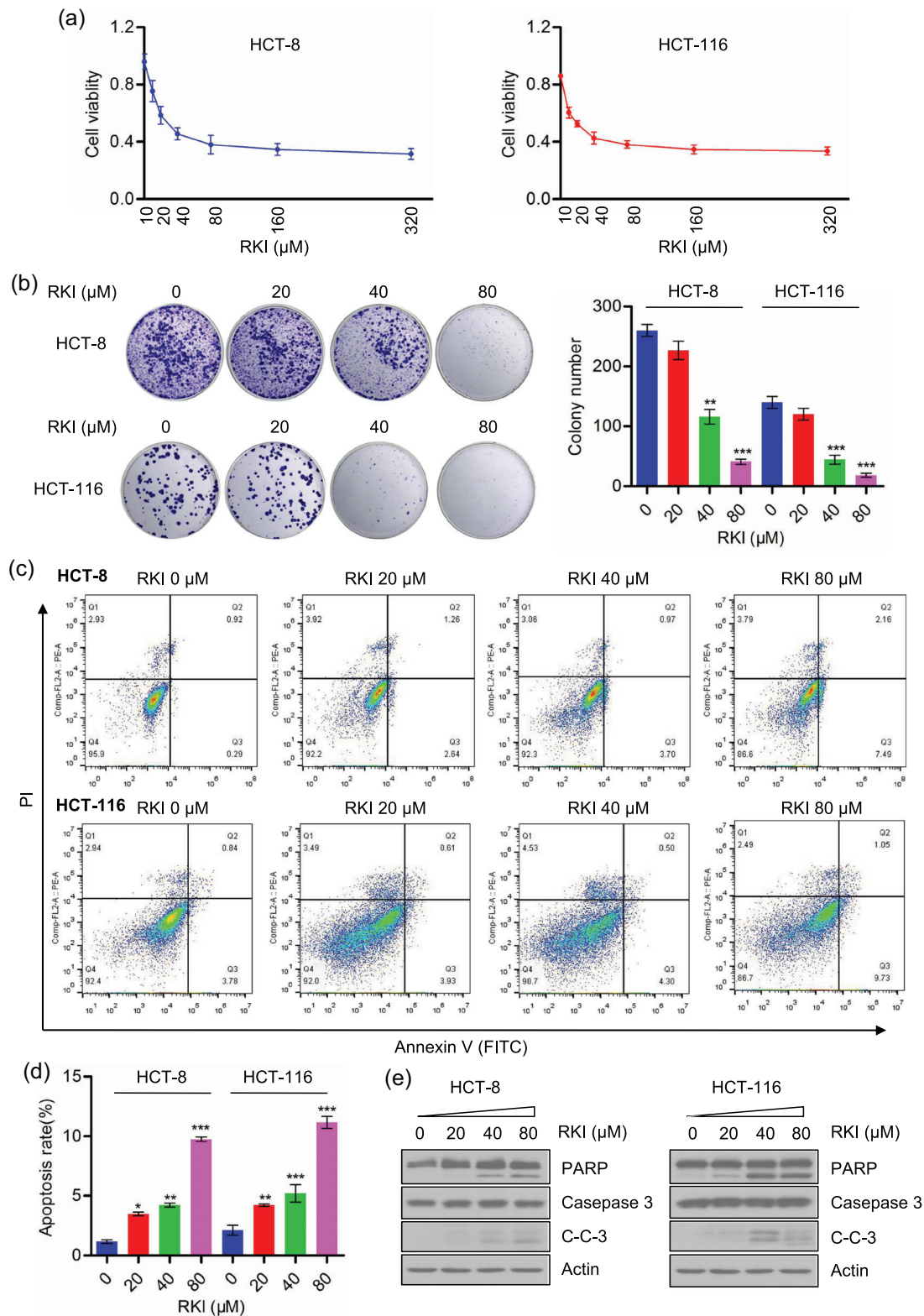


FIGURE 1 RKI-1447 effectively suppresses CRC cell growth. (a) HCT-8 and HCT-116 cells were treated with a gradient concentration of RKI-1447 (0, 10, 20, 40, 80, 160, 320 μM) for 24 hr. Cell viability was determined by the MTT assay. (b) HCT-8 and HCT-116 cells were seeded into six-well plates, and cultured with RKI-1447 (0, 20, 40, 80 μM) for 14 days. Giemsa solution was used to visualize colonies, and colony number were counted and quantified. (c) HCT-8 and HCT-116 cells were treated with different concentrations of RKI-1447 (0, 20, 40, 80 μM) for 24 hr followed by flow cytometry analysis to determine cell apoptotic rate. (d) Quantitative data of RKI-1447 induced HCT-8 and HCT-116 cell apoptosis. (e) HCT-8 and HCT-116 cells were treated with different concentrations of RKI-1447 (0, 20, 40, 80 μM) for 24 hr, and the cell samples were collected, followed by western blot analysis with indicated antibodies. The data shown are mean ± SD. (** $p < .01$, *** $p < .001$, by Student's t test) [Color figure can be viewed at wileyonlinelibrary.com]

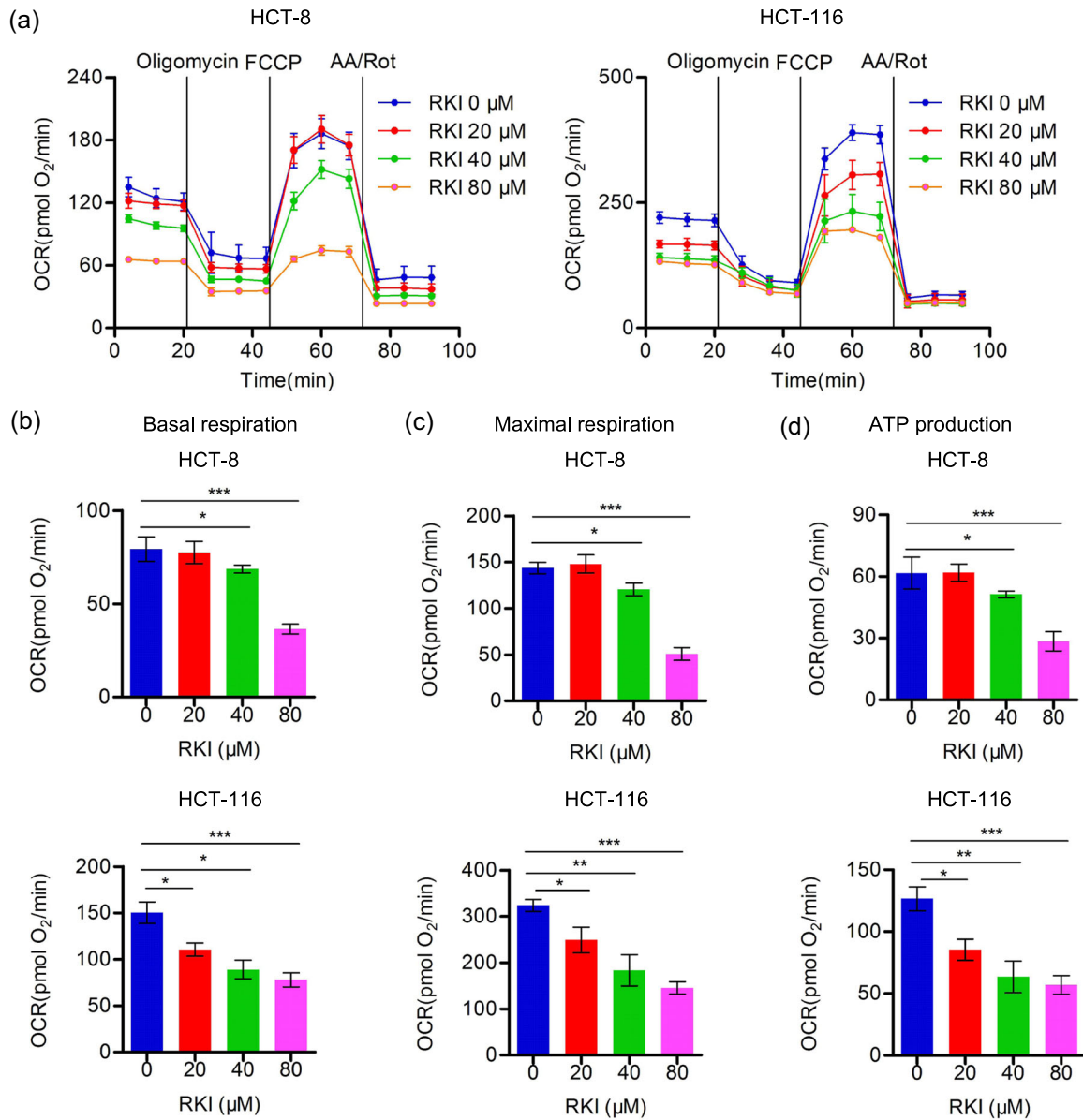


FIGURE 2 RKI-1447 drastically inhibits mitochondrial respiration. (a) Real time overall OCR of HCT-8 and HCT-116 cells treated with RKI-1447 of different concentrations for 24 hr was detected by seahorse XF96 cellular bioenergetics analyzer. (b) Basal respiration rate, (c) Maximal respiration rate, and (d) ATP production associated OCR of HCT-8 and HCT-116 cells treated by RKI-1447 of various concentrations. Each group included at least three replicates. OCR, oxygen consumption rate. The data shown are mean \pm SD. (** $p < .01$, ** $p < .01$, *** $p < .001$) [Color figure can be viewed at wileyonlinelibrary.com]

3.5 | Upregulation CHOP is essential for RKI-1447 induced cell apoptosis but not cellular bioenergetics

To further confirm the effects of RKI-1447 on cell viability and ER stress activation, we knockout ROCK1 in HCT-8 cells and detected cell viability, ROS generation, and membrane potential and ER stress associated molecules. The data showed in ROCK1 depleted cells, cell viability was significantly reduced and ROS level was increased (Figure S2a,b). Membrane potential data showed ROCK1 knockout remarkably caused mitochondrial depolarization Figure 2c). To further understand the effects of ROCK1 depletion on ER stress activation, we depleted ROCK

and found activated OPA1 cleavage and upregulated ER stress associated molecules in ROCK1 knockout cells (Figure 3). We evaluated the effects of activated CHOP on cell viability and cell apoptosis. We found siRNA targeting CHOP could dramatically alleviate RKI-1447 caused cell apoptosis by flow cytometry and caspase 3 activity assay (Figure 5a–c). Consistently, we found knockdown CHOP in RKI-1447 treated cells could significantly attenuate the tumor-suppressive activity of RKI-1447 (Figure 5d). These data indicated that upregulation of CHOP may responsible for RKI-1447 delayed cancer cell growth. However, no significance of ROS and MMP was found in CHOP depletion cells, suggesting that mitochondrial disruption maybe the upstream of CHOP

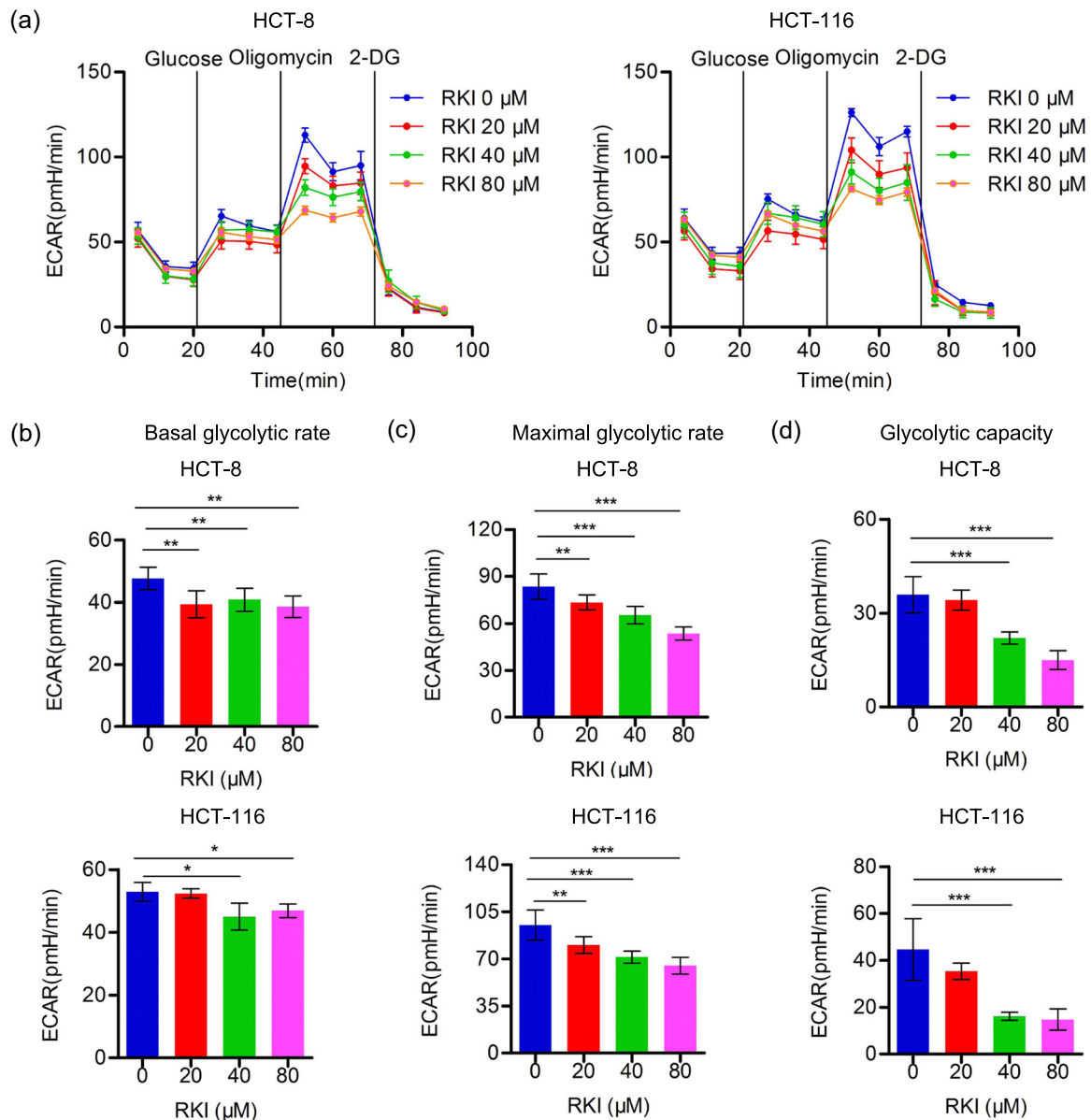


FIGURE 3 RKI-1447 significantly represses cellular aerobic glycolysis. (a) Real time overall ECAR of HCT-8 and HCT-116 cells treated with RKI-1447 of various concentrations for 24 hr was detected by seahorse XF96 cellular bioenergetics analyzer. (b) Basal glycolytic rate, (c) Maximal glycolytic rate, and (d) Glycolytic capacity of HCT-8 and HCT-116 cells treated by RKI-1447 of various concentrations. ECAR, extracellular acidification rate. Each group included at least three replicates. The data shown are mean \pm SD. (** $p < .01$, ** $p < .01$, *** $p < .001$) [Color figure can be viewed at wileyonlinelibrary.com]

activation (Figure 5e,f). Interestingly, we found silencing of CHOP in RKI-1447 treated cells could not rescue RKI-1447 caused reduction of mitochondrial respiration (Figure 5g). Spontaneously, ECAR upon oligomycin addition could slightly recovered by CHOP knockdown (Figure 5h). These data indicated CHOP maybe responsible for RKI-1447 caused cell apoptosis, but not the cellular bioenergetics.

3.6 | RKI-1447 exerts antitumor activity on CRC in vivo

To further confirm the antitumor activity of RKI-1447, we used Balb/C nude mice to investigate the activity of RKI-1447 in vivo. We

subcutaneously injected HCT-8 cells into nude mice and measured subsequent change in body weight and tumor volume. Once the tumor volume grew to 250 mm^3 , the mice were divided into two cohorts. One group was injected with 0.9% NaCl vehicle, and another was injected with RKI-1447 (100 mg/kg), once every 3 days. At the end of the treatment, tumor tissues were resected and imaged. As shown in Figure 6a, the tumor tissues were smaller in RKI-1447 treated group compare to those in vehicle treated group. Body weight showed no significant difference between these two groups, which indicated that this dose of RKI-1447 did not exert physiological toxicity on the mice (Figure 6b). We also measured tumor weight of both groups, and found tumor weight was significantly

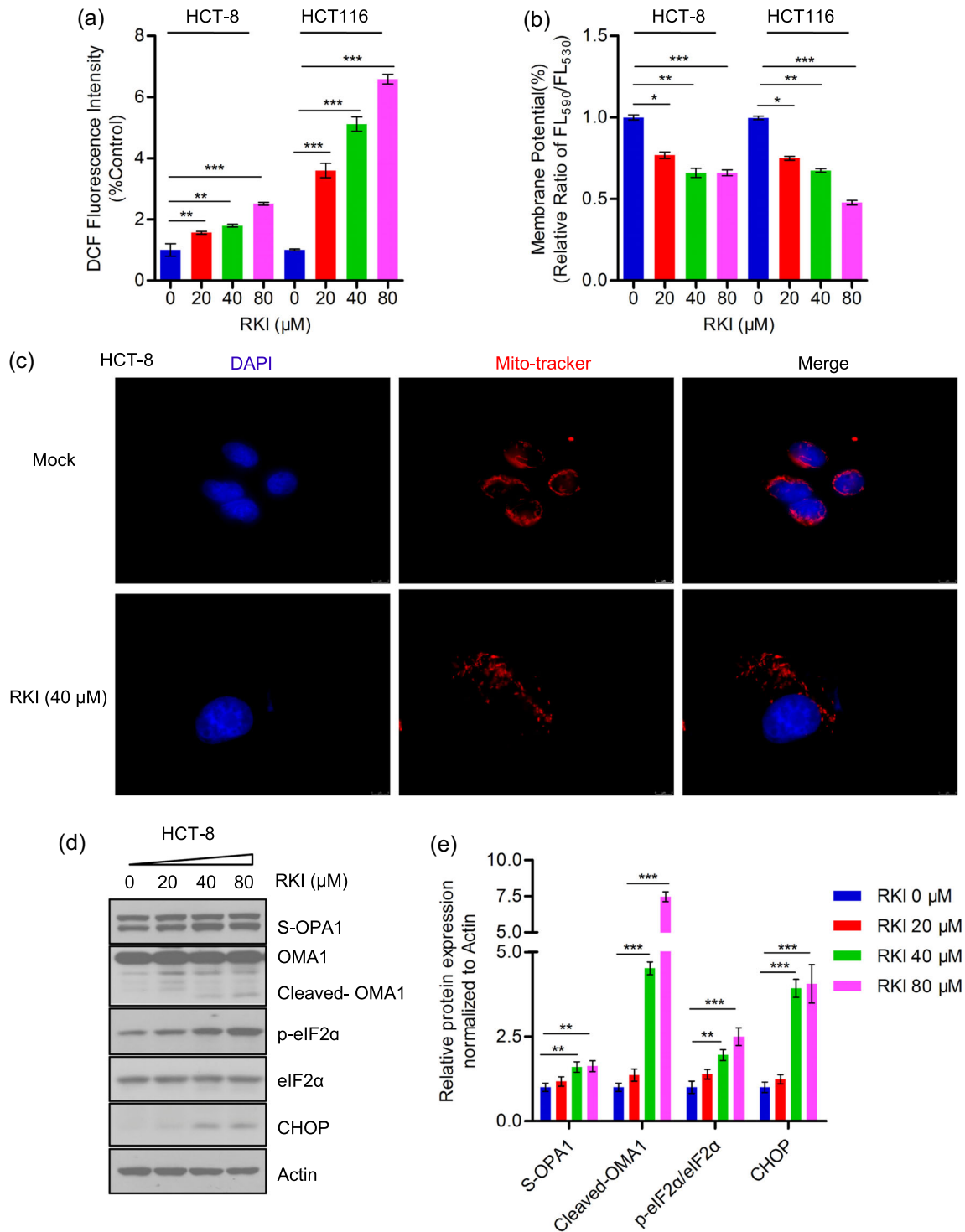


FIGURE 4 RKI-1447 promotes ROS production and activates ER-stress. (a) HCT-8 and HCT-116 cells were treated by RKI-1447 (0, 20, 40, 80 μM) for 24 hr, total cellular ROS level was detected by DCFH-DA kit and analyzed by flow cytometry. (b) Mitochondrial membrane potential alteration of HCT-8 and HCT-116 cells in response to RKI-1447 treatment. (c) HCT-8 cells were treated with RKI-1447 (40 μM) for 24 hr, and then stained with DAPI and mitotracker. The images were captured by fluorescence microscope. (d) HCT-8 cells were treated with RKI-1447 (0, 20, 40, 80 μM) for 24 hr, the cellular proteins were subjected to western blot analysis with indicated antibodies. (e) Quantitative data of protein level of Figure 4d. ROS, reactive oxygen species. The data shown are mean ± SD. (***p* < .01, ****p* < .001) [Color figure can be viewed at wileyonlinelibrary.com]

reduced upon RKI-1447 treatment (Figure 6c). Consistently, tumor growth curve also showed RKI-1447 drastically suppressed CRC growth in vivo (Figure 6d). We also investigated OPA1 and OMA1 cleavage, p-eIF2α and CHOP levels in tumor tissues. As shown in

Figure 5e, increased cleavage of OPA1 and OMA1, increased p-eIF2α and CHOP expression were found in RKI-1447 treated groups which were consistent with data in cell line studies. These data indicated that RKI-1447 exert antitumor activity on CRC in vivo.

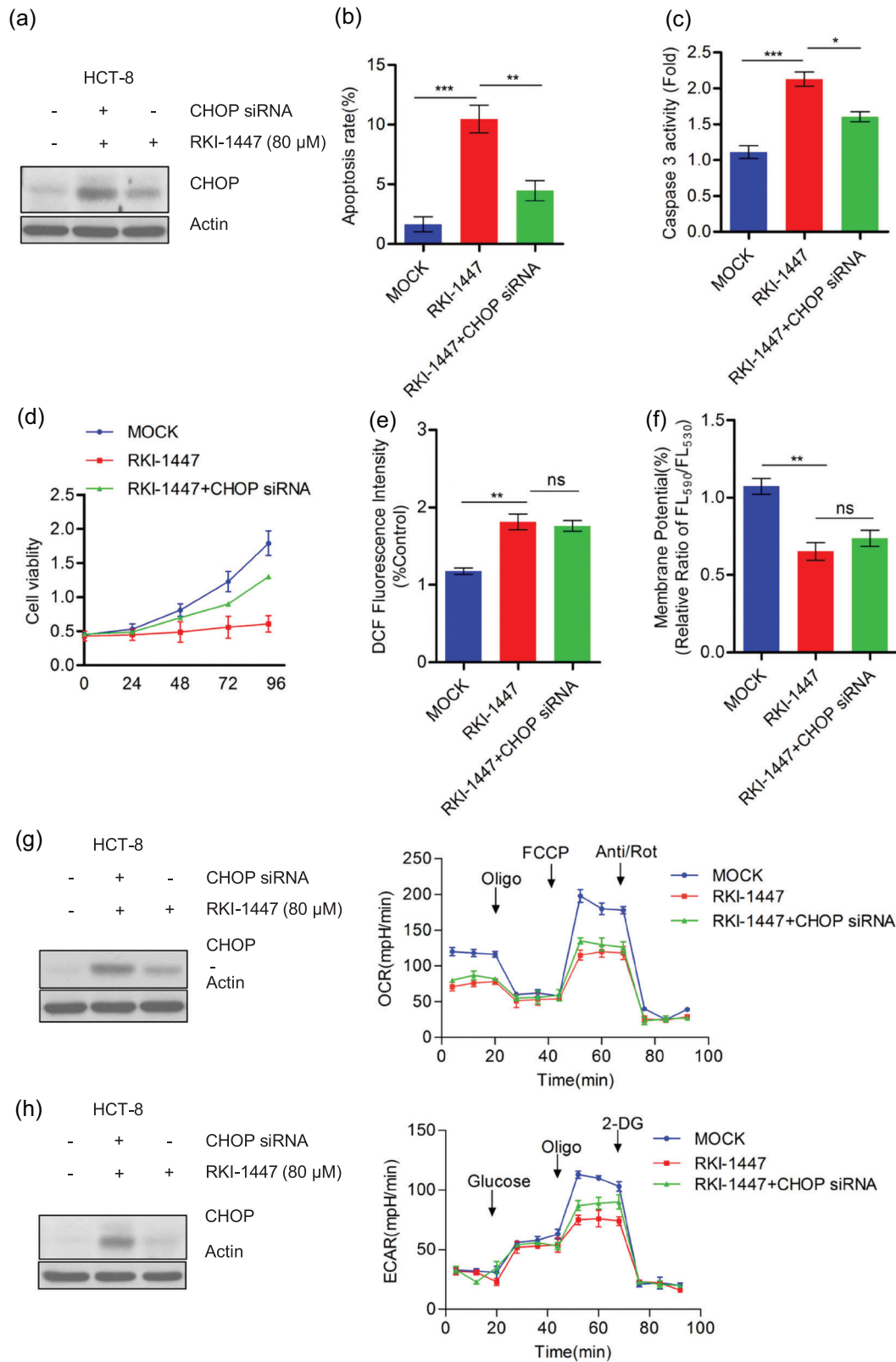


FIGURE 5 CHOP is indispensable for RKI-1447 induced cell apoptosis. (a) Western blot data of CHOP level in RKI-1447 cells. (b) Apoptotic cells in MOCK, RKI-1447, RKI-1447 combined with CHOP siRNA HCT-8 cells were detected flow cytometry analysis. (c) caspase enzyme activity was determined by caspase activity detection kit. (d) The cell viability of MOCK, RKI-1447, RKI-1447 combined with CHOP siRNA treated cells were evaluated by MTT assay. (e,f) Total ROS level and MMP were assessed by flow cytometry. (g,h) MOCK, RKI-1447, RKI-1447 combined with CHOP siRNA treated cells were subjected to the cellular bioenergetics analysis to detect OCR and ECAR. The data shown are mean \pm SD. ECAR, extracellular acidification rate; OCR, oxygen consumption rate. (** $p < .01$, *** $p < .01$, **** $p < .001$) [Color figure can be viewed at wileyonlinelibrary.com]

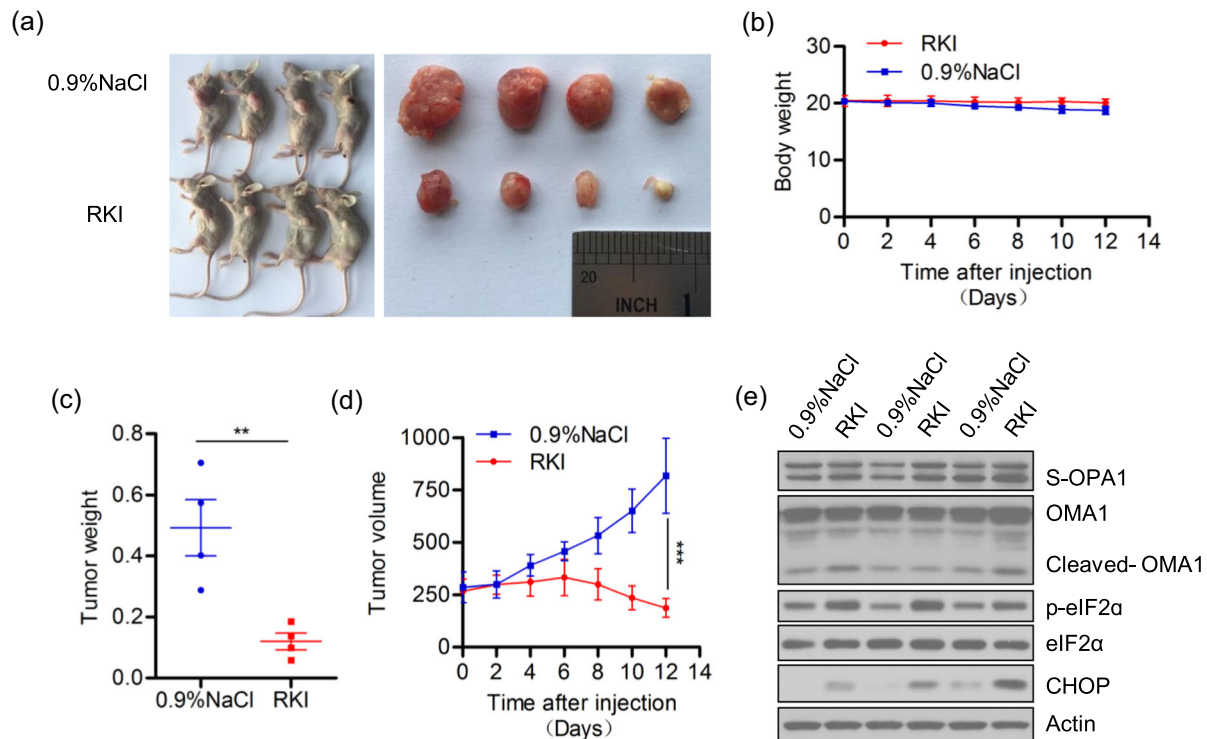


FIGURE 6 RKI-1447 efficiently blocks CRC tumor growth in vivo. (a) Images of nude mice administrated with 0.9% NaCl or RKI-1447 (100 mg/kg) and corresponding tumors sections. (b) Body weight of nude mice treated with 0.9% NaCl or RKI-1447. (c) Tumor weight of 0.9% NaCl or RKI-1447 treated CRC tumors. (d) Growth of tumors in 0.9% NaCl or RKI-1447 treated nude mice. (E) Tumor sections were homogenized and protein extracts subjected to western blot analysis with indicated antibodies. The data shown are mean \pm SEM. CRC, colorectal carcinoma. (** $p < .01$, *** $p < .001$) [Color figure can be viewed at wileyonlinelibrary.com]

4 | DISCUSSION

ROCK1/2 associated signaling is associated with cancer growth and metastasis, such as breast cancer, gastric cancer, and ovarian cancer (Bhandary et al., 2015; Matsuoka & Yashiro, 2014; Pettee, Dvorak, Nestor-Kalinoski, & Eisenmann, 2014). Recently, growing evidence demonstrated that ROCK1/2 signaling plays crucial roles in invasion and metastasis of CRC (Bottino, Gelaleti, Maschio, Jardim-Perassi, & de Campos Zuccari, 2014; Patel et al., 2014; Voorneveld et al., 2014; Zeng et al., 2015). Ablation of ROCK1/2 function was validated to effectively suppress tumor growth and survival (Jin et al., 2016; Li et al., 2013; Yao, Gao, Xu, & Li, 2016). RKI1447, a novel ROCK1/2 inhibitor was demonstrated to repress ROCK1/2 dependent tumor growth, migration and invasion in breast cancer and clear cell renal cell carcinoma (Patel et al., 2012; Thompson et al., 2017). However, the impact of RKI-1447 on CRC remains unknown. In the current study, we found RKI-1447 could drastically suppress CRC cell growth and promote apoptosis in vitro and in vivo. All these highlight the anticancer activity of RKI-1447 in CRC.

It is well demonstrated that tumor cells need more energy and metabolic intermediates to sustain rapid proliferation. By phosphorylating mitochondrial DRP1, ROCK has been demonstrated to affect mitochondrial function. Mitochondria respiration and aerobic glycolysis processes are crucial for the production of ATP and metabolic

intermediates. Here, we found ROCK1/2 inhibition by RKI-1447 remarkably disrupted cellular bioenergetics through downregulating mitochondrial respiration and aerobic glycolysis. This indicated the potential role of ROCK1/2 in regulating cellular bioenergetics. Further work is needed to investigate the role of ROCK1/2 in regulating these two processes, and whether the effect of RKI-1447 is caused by ROCK1/2 inhibition. Furthermore, we found excessive ROS generation and mitochondrial depolarization upon RKI-1447 treatment, which further confirmed the effects of RKI-1447 on mitochondrial dysfunction. So we suggest that RKI-1447 induced cellular bioenergetics suppression probably contributes to CRC tumor cell growth arrest and promotion of apoptosis.

Previous works have demonstrated the close association between ER and mitochondria. Disruption of mitochondria and ER connection plays critical roles in many pathophysiological processes (Horner, Wilkins, Badil, Iskarpatyoti, & Gale, 2015; Lee & Yoon, 2014; Murley et al., 2013; Sun et al., 2015). As described above, RKI-1447 promoted ROS generation, mitochondrial depolarization and mitochondrial fragmentation which would interrupt the interaction between ER and mitochondria. OPA1, a key protein in regulating mitochondrial dynamics, was cleaved to S-OPA1 by OMA1 upon RKI-1447 treatment. OPA1 cleavage was found to disturb the association between ER and mitochondria, which probably activates ER stress (Li, Zhu, Fang, Jiang, & Tang, 2014; Liu et al., 2014; Namba & Kodama,

2015). In the current study, we demonstrated RKI-1447 caused mitochondrial dysfunction and promoted cleavage of OPA1. Previous work has validated increased S-OPA1 would further result in mitochondrial fragmentation as well as activating ER stress. Moreover, there are contacts between mitochondria and ER which is named Mitochondria-associated ER membranes (MAM). MAM linkage consists of some proteins and an ER region containing lipid biosynthetic enzyme. It is a mechanism which enables communication between endoplasmic reticulum (ER) and mitochondria. MAM is connected reversibly to mitochondria, and plays crucial role in calcium homeostasis, regulation of lipid metabolism, regulation of autophagy and mitophagy, mitochondrial dynamics and functions, and cell survival (Marchi, Patergnani, & Pinton, 2014; Polo et al., 2017; Rowland & Voeltz, 2012). So we speculated that RKI-1447 caused mitochondrial disruption and destroyed the integrity of MAM which further activated ER stress. Further work may focus on elucidating the molecular mechanism of MAM alteration in response to RKI-1447 treatment. It was well validated that activation of p-PERK-p-eif2 α -ATF4-CHOP signaling transduction would promote transcription of apoptosis associated genes, which finally induce apoptosis (B'chir et al., 2014). So we propose that RKI-1447 treatment causes mitochondrial dysfunction, which promotes ROS generation and restricts bioenergetics processes. Meanwhile, RKI-1447 activates OPA-1 cleavage, which disrupts MAM and induces ER stress. The processes above finally induce cell apoptosis and suppress CRC cell growth. CHOP and p-eIF2 α were demonstrated to be a crucial factor in promoting apoptosis. In this study, we demonstrated CHOP is indispensable for RKI-1447 induced cell apoptosis, but not contributes to cellular bioenergetics disruption. Further work is needed to clarify the intrinsic mechanism of RKI-1447 activated ER stress and CHOP-p-eIF2 α -mediated apoptosis.

Collectively, we propose RKI-1447 suppresses CRC tumor growth through disruption of mitochondrial homeostasis, which enhances oxidative damage and represses cellular bioenergetics. Simultaneously, mitochondrial dysfunction interrupts the crosstalk between ER and mitochondria, which subsequently activates ER stress and promotes CHOP-p-eIF2 α mediated apoptosis. These data suggest that RKI-1447 could be considered as a promising candidate for CRC therapy.

ACKNOWLEDGMENTS

We thank Dr. Yong Ai for the helpful discussions and suggestions of this manuscript and we also thank Tongke Chen for the help with the xenograft tumor growth assay. This work was supported by grant from Key Research and Development Program of Shandong Province (No. 2015GGH318017).

CONFLICT OF INTEREST

The authors declare that there is no conflict of interest

AUTHOR CONTRIBUTIONS

L. Y. L. and H. C. conceived and designed the experiments. L. Y. L., H. C., M. D. L., Y. P. H., and P. H. L. performed the experiments. L. Y. and H. C. coordinated the research and analyzed the data. H. C., M. D. L., and Y. P. H. helped to draft the manuscript. L. Y. L. and H. C. performed the statistical analysis. L. Y. L. and H. C. wrote the manuscript. All authors read and approved the final manuscript.

ETHICAL APPROVAL

The in vivo experiments were performed in accordance with the guidelines of the Institutional Animal Care and Use Committee, and this study was approved by The Tab of Animal Experimental Ethical Inspection of Laboratory Animal Centre, Wenzhou Medical University

DATA AVAILABILITY STATEMENT

The data used to support the findings of this study are available from the corresponding author upon request.

ORCID

Liyi Li  <http://orcid.org/0000-0003-0809-6388>

REFERENCES

- Alessi, D. R., & Cohen, P. (1998). Mechanism of activation and function of protein kinase B. *Current Opinion in Genetics & Development*, 8(1), 55–62.
- B'chir, W., Chaveroux, C., Carraro, V., Averous, J., Maurin, A. C., Jousse, C., ... Bruhat, A. (2014). Dual role for CHOP in the crosstalk between autophagy and apoptosis to determine cell fate in response to amino acid deprivation. *Cellular Signalling*, 26(7), 1385–1395.
- Banerjee, S., & Chinthapalli, B. (2014). A proteomic screen with *Drosophila* Opa1-like identifies Hsc70-5/Mortalin as a regulator of mitochondrial morphology and cellular homeostasis. *International Journal of Biochemistry and Cell Biology*, 54, 36–48.
- Bhandary, L., Whipple, R. A., Vitolo, M. I., Charpentier, M. S., Boggs, A. E., Chakrabarti, K. R., ... Martin, S. S. (2015). ROCK inhibition promotes microtubules that enhance reattachment of breast cancer cells. *Oncotarget*, 6(8), 6251–6266.
- Bottino, J., Galaleti, G. B., Maschio, L. B., Jardim-Perassi, B. V., & deCampos Zuccari, D. A. (2014). Immunoeexpression of ROCK-1 and MMP-9 as prognostic markers in breast cancer. *Acta Histochemica*, 116(8), 1367–1373.
- Chen, X. Q., Tan, I., Ng, C. H., Hall, C., Lim, L., & Leung, T. (2002). Characterization of RhoA-binding kinase ROKalpha implication of the pleckstrin homology domain in ROKalpha function using region-specific antibodies. *Journal of Biological Chemistry*, 277(15), 12680–12688.
- Di Cunto, F., Imarisio, S., Hirsch, E., Broccoli, V., Bulfone, A., Migheli, A., ... Altruda, F. (2000). Defective neurogenesis in citron kinase knockout mice by altered cytokinesis and massive apoptosis. *Neuron*, 28(1), 115–127.
- Ferlay, J., Soerjomataram, I., Dikshit, R., Eser, S., Mathers, C., Rebelo, M., ... Bray, F. (2015). Cancer incidence and mortality worldwide: Sources, methods and major patterns in GLOBOCAN 2012. *International Journal of Cancer*, 136(5), E359–E386.

- Gemma, Binefa, & Francisco, et al. (2014). Colorectal cancer: From prevention to personalized medicine. *World Journal of Gastroenterology*, 20(22), 6786–6808.
- Horner, S. M., Wilkins, C., Badil, S., Iskarpatyoti, J., & Gale, M., Jr. (2015). Proteomic analysis of mitochondrial-associated ER membranes (MAM) during RNA virus infection reveals dynamic changes in protein and organelle trafficking. *PLoS One*, 10(3), e0117963.
- Jin, S., Shimizu, M., Balasubramanyam, A., Epstein, & H, F. (2000). Myotonic dystrophy protein kinase (DMPK) induces actin cytoskeletal reorganization and apoptotic-like blebbing in lens cells. *Cell Motil. Cytoskeleton*, 45(2), 133–148.
- Jin, X., Liu, K., Jiao, B., Wang, X., Huang, S., Ren, W., ... Zhao, K. (2016). Vincristine promotes migration and invasion of colorectal cancer HCT116 cells through RhoA/ROCK/ Myosin light chain pathway. *Cellular and Molecular Biology*, 62(12), 91–96.
- Kushnareva, Y. E., Gerencser, A. A., Bossy, B., Ju, W. K., White, A. D., Waggoner, J., ... Bossy-Wetzels, E. (2013). Loss of OPA1 disturbs cellular calcium homeostasis and sensitizes for excitotoxicity. *Cell Death and Differentiation*, 20(2), 353–365.
- Lee, H., & Yoon, Y. (2014). Mitochondrial fission: Regulation and ER connection. *Molecules and Cells*, 37(2), 89–94.
- Leung, T., Chen, X.-Q., Manser, E., & Lim, L. (1996). The p160 RhoA-binding kinase ROK alpha is a member of a kinase family and is involved in the reorganization of the cytoskeleton. *Molecular and Cellular Biology*, 16(10), 5313–5327.
- Leung, T., Chen, X.-Q., Tan, I., Manser, E., & Lim, L. (1998). Myotonic dystrophy kinase-related Cdc42-binding kinase acts as a Cdc42 effector in promoting cytoskeletal reorganization. *Molecular and Cellular Biology*, 18(1), 130–140.
- Li, H., Zhu, X., Fang, F., Jiang, D., & Tang, L. (2014). Down-regulation of GRP78 enhances apoptosis via CHOP pathway in retinal ischemia-reperfusion injury. *Neuroscience Letters*, 575, 68–73.
- Li, N., Tang, A., Huang, S., Li, Z., Li, X., Shen, S., ... Wang, X. (2013). MiR-126 suppresses colon cancer cell proliferation and invasion via inhibiting RhoA/ROCK signaling pathway. *Molecular and Cellular Biochemistry*, 380(1–2), 107–119.
- Liberti, M. V., & Locasale, J. W. (2016). The Warburg Effect: How does it benefit cancer cells? *Trends in Biochemical Sciences*, 41(3), 211–218.
- Liu, K., Shi, Y., Guo, X., Wang, S., Ouyang, Y., Hao, M., ... Chen, D. (2014). CHOP mediates ASP2-induced autophagic apoptosis in hepatoma cells by releasing Beclin-1 from Bcl-2 and inducing nuclear translocation of Bcl-2. *Cell Death & Disease*, 5, e1323–e1323.
- Ly, J. D., Grubb, D. R., & Lawen, A. (2003). The mitochondrial membrane potential ($\Delta\psi(m)$) in apoptosis; an update. *Apoptosis*, 8(2), 115–28.
- Madaule, P., Eda, M., Watanabe, N., Fujisawa, K., Matsuoka, T., Bito, H., ... Narumiya, S. (1998). Role of citron kinase as a target of the small GTPase Rho in cytokinesis. *Nature*, 394(6692), 491–494.
- Marchi, S., Patergnani, S., & Pinton, P. (2014). The endoplasmic reticulum-mitochondria connection: One touch, multiple functions. *Biochimica et Biophysica Acta*, 1837, 461–469.
- Matsuoka, T., & Yashiro, M. (2014). Rho/ROCK signaling in motility and metastasis of gastric cancer. *World Journal of Gastroenterology*, 20(38), 13756–13766.
- Matés, J. M., Segura, J. A., Alonso, F. J., & Márquez, J. (2012). Oxidative stress in apoptosis and cancer: An update. *Archives of Toxicology*, 86(11), 1649–1665.
- Murley, A., Lackner, L. L., Osman, C., West, M., Voeltz, G. K., Walter, P., ... Nunnari, J. (2013). ER-associated mitochondrial division links the distribution of mitochondria and mitochondrial DNA in yeast. *eLife*, 2, e00422.
- Namba, T., & Kodama, R. (2015). Avarol induces apoptosis in pancreatic ductal adenocarcinoma cells by activating PERK-eIF2 α -CHOP signaling. *Marine Drugs*, 13(4), 2376–2389.
- Newton, A. C. (1997). Regulation of protein kinase C. *Current Opinion in Cell Biology*, 9(2), 161–167.
- Patel, M., Kawano, T., Suzuki, N., Hamakubo, T., Karginov, A. V., & Kozasa, T. (2014). G α 13/PDZ-RhoGEF/RhoA signaling is essential for gastrin-releasing peptide receptor-mediated colon cancer cell migration. *Molecular Pharmacology*, 86(3), 252–262.
- Patel, R. A., Forinash, K. D., Pireddu, R., Sun, Y., Sun, N., Martin, M. P., ... Sebti, S. M. (2012). RKI-1447 is a potent inhibitor of the Rho-associated ROCK kinases with anti-invasive and antitumor activities in breast cancer. *Cancer Research*, 72(19), 5025–5034.
- Pettee, K. M., Dvorak, K. M., Nestor-Kalinoski, A. L., & Eisenmann, K. M. (2014). An mDia2/ROCK signaling axis regulates invasive egress from epithelial ovarian cancer spheroids. *PLoS One*, 9(2), e90371.
- Poillet-Perez, L., Despouy, G., Delage-Mourroux, R., & Boyer-Guittaut, M. (2015). Interplay between ROS and autophagy in cancer cells, from tumor initiation to cancer therapy. *Redox Biology*, 4, 184–192.
- Polo, M., Alegre, F., Moragrega, A. B., Gibellini, L., Marti-Rodrigo, A., Blas-Garcia, A., ... Apostolova, N. (2017). Lon protease: A novel mitochondrial matrix protein in the interconnection between drug-induced mitochondrial dysfunction and endoplasmic reticulum stress. *British Journal of Pharmacology*, 174, 4409–4429.
- Quiros, P. M., Ramsay, A. J., & López-Otín, C. (2013). New roles for OMA1 metalloprotease: From mitochondrial proteostasis to metabolic homeostasis. *Adipocyte*, 2(1), 7–11.
- Riento, K., & Ridley, A. J. (2003). Rocks: Multifunctional kinases in cell behaviour. *Nature Reviews Molecular Cell Biology*, 4(6), 446–456.
- Rowland, A. A., & Voeltz, G. K. (2012). Endoplasmic reticulum-mitochondria contacts: Function of the junction. *Nature Reviews Molecular Cell Biology*, 13, 607–625.
- Stefano, G. B., & Kream, R. M. (2015). Cancer: Mitochondrial origins. *Medical Science Monitor*, 21, 3736–3739.
- Sun, Q., Zhong, W., Zhang, W., Li, Q., Sun, X., Tan, X., ... Zhou, Z. (2015). Zinc deficiency mediates alcohol-induced apoptotic cell death in the liver of rats through activating ER and mitochondrial cell death pathways. *American journal of Physiology. Gastrointestinal and liver physiology*, 308(9), G757–G766.
- Suzuki-Karasaki, Y., Suzuki-Karasaki, M., & Uchida, M. (2014). Ochiai T2. depolarization controls TRAIL-sensitization and tumor-selective killing of cancer cells: Crosstalk with ROS. *Frontiers in Oncology*, 4, 128.
- Thompson, J. M., Nguyen, Q. H., Singh, M., Pavesic, M. W., Nesterenko, I., Nelson, L. J., ... Razorenova, O. V. (2017). Rho-associated kinase 1 inhibition is synthetically lethal with von Hippel-Lindau deficiency in clear cell renal cell carcinoma. *Oncogene*, 36(8), 1080–1089.
- Vanhaesebroeck, B., & Alessi, D. R. (2000). The PI3K-PDK1 connection: More than just a road to PKB. *Biochemical Journal*, 346(Pt3), 561–576.
- Vega, F. M., & Ridley, A. J. (2008). Rho GTPases in cancer cell biology. *FEBS Letters*, 582(14), 2093–2101.
- Voorneveld, P. W., Kodach, L. L., Jacobs, R. J., Liv, N., Zonneville, A. C., Hoogenboom, J. P., ... Hardwick, J. C. H. (2014). Loss of SMAD4 alters BMP signaling to promote colorectal cancer cell metastasis via activation of Rho and ROCK. *Gastroenterology*, 147(1), 196–208.
- Vyas, S., Zaganjor, E., & Haigis, M. C. (2016). Mitochondria and cancer. *Cell*, 166(3), 555–566.
- Wang, W., Wang, Y., Long, J., Wang, J., Haudek, S., Overbeek, P., ... Danesh, F. (2012). Mitochondrial fission triggered by hyperglycemia is mediated by ROCK1 activation in podocytes and endothelial cells. *Cell Metabolism*, 15(2), 186–200.
- Wang, J., Zhang, B., Wu, H., Cai, J., Sui, X., Wang, Y., ... Xiang, A. P. (2017). CD51 correlates with the TGF-beta pathway and is a functional marker for colorectal cancer stem cells. *Oncogene*, 36(10), 1351–1363.
- Shi, Y., Fan, S., Wang, D., Huyan, T., Chen, J., Chen, J., ... Tie, L. (2018). FOXO1 inhibition potentiates endothelial angiogenic functions in diabetes via suppression of ROCK1/Drp1-mediated mitochondrial

- fission. *Bbadis*, 1864, 2481–2494. <https://doi.org/10.1016/j.bbadis.2018.04.005>
- Yao, J., Gao, P., Xu, Y., & Li, Z. (2016). α -TEA inhibits the growth and motility of human colon cancer cells via targeting RhoA/ROCK signaling. *Molecular Medicine Reports*, 14(3), 2534–2540.
- Zeng, Y., Xie, H., Qiao, Y., Wang, J., Zhu, X., He, G., ...Ding, Y. (2015). Formin-like2 regulates Rho/ROCK pathway to promote actin assembly and cell invasion of colorectal cancer. *Cancer Science*, 106(10), 1385–1393.
- Zhang, D., Lu, C., Whiteman, M., Chance, B., & Armstrong, J. S. (2008). The mitochondrial permeability transition regulates cytochrome c release for apoptosis during endoplasmic reticulum stress by remodeling the cristae junction. *Journal of Biological Chemistry*, 283(6), 3476–3486.

SUPPORTING INFORMATION

Additional supporting information may be found online in the Supporting Information section.

How to cite this article: Li L, Chen Q, Yu Y, et al. RKI-1447 suppresses colorectal carcinoma cell growth via disrupting cellular bioenergetics and mitochondrial dynamics. *J Cell Physiol*. 2019;1–13. <https://doi.org/10.1002/jcp.28965>